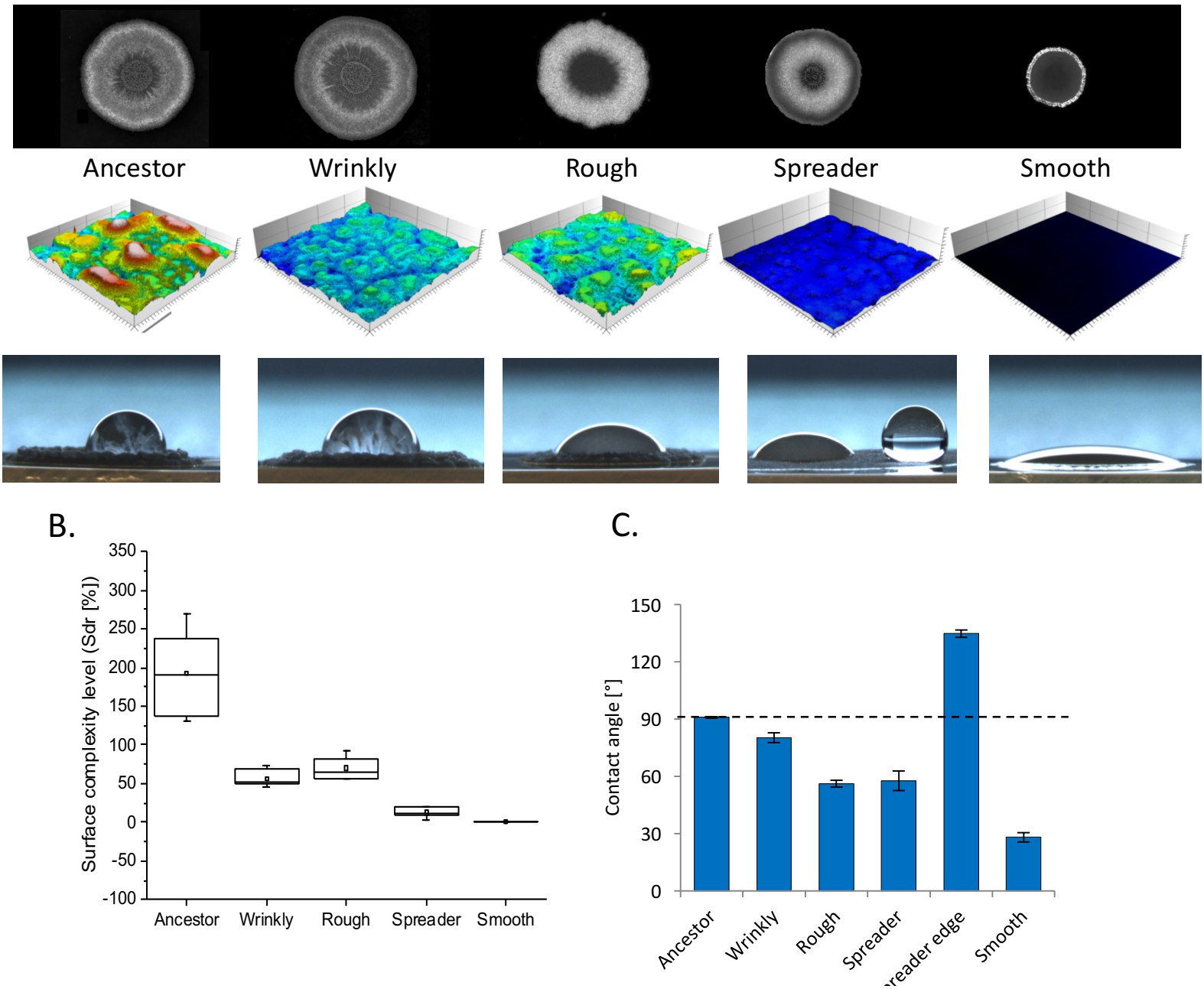

Supplementary Figure S1. Morphotypes morphology on MSgg and quantitative characterization of their colony features displayed on rich LB medium. **(A)** Colony morphologies of the ancestor and four distinct morphotypes spotted on MSgg medium (1.5% agar) are shown above. Middle, the surface topologies of the colonies developed on LB medium. Surface topologies of the ancestor and evolved morphotypes were acquired using light profilometry. 3D images of the surface topology were generated using the software µsurf (see methods) showing topological features with a standard color scale- where dark blue represents the lowest and white represents the highest features. Colonies were grown for 48h at 30°C. Scale bar represents 200µm. Below, image of 10µl water droplet spotted in the center, or colony periphery in case of the Spreader morphotype. **(B)** Developed interfacial area *Sdr* calculated for colony center of the ancestor and four morphotypes (n=6 or n=5) for colonies grown on LB medium. Boxes represent Q1–Q3, lines represent the median, small squares represent the mean and bars span from max to min. **(C)** Contact angles of water spotted in the colony center, or colony periphery in case of the Spreader (n=3) for colonies grown on LB medium. Dashed line represents contractual hydrophobicity cut-off, separating the surfaces on hydrophilic (below the line) and hydrophobic (above). Data points represent mean and error bars represent standard error.

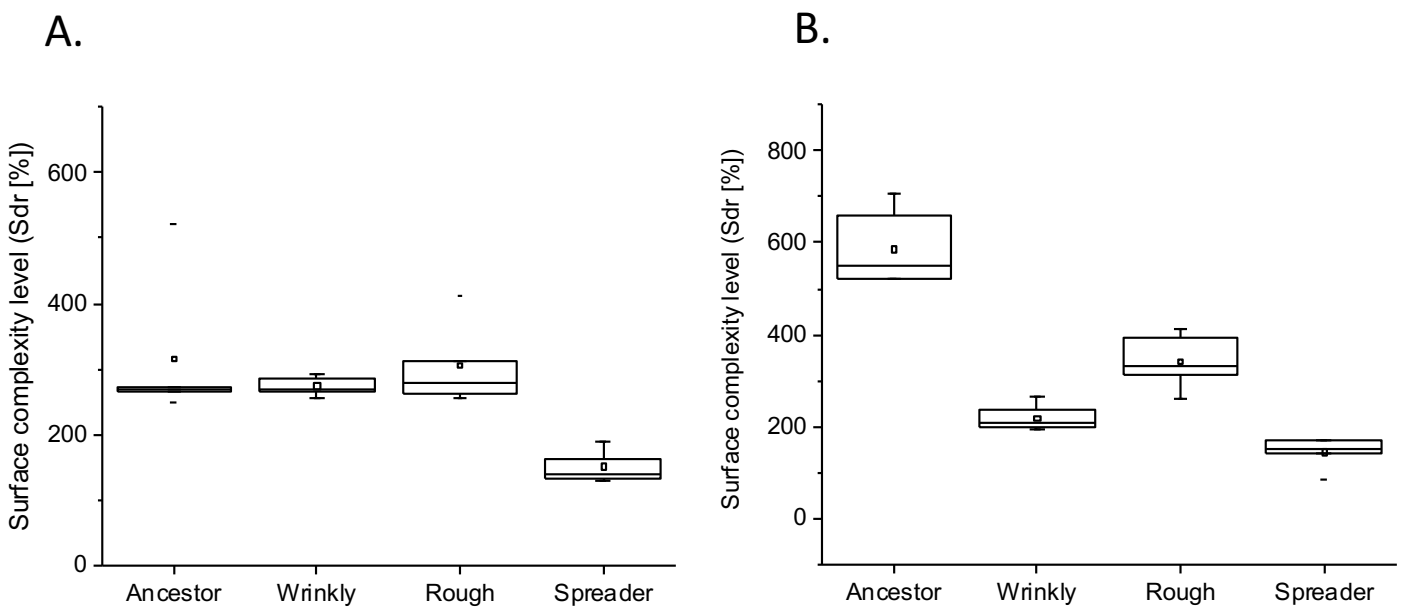

Supplementary Figure S2. Characterization of colony surface profiles at colony periphery. **(A)** Developed interfacial area *Sdr* calculated for colony periphery for colonies developed on MSgg medium (n=6 or n=5). **(B)** Developed interfacial area *Sdr* calculated for colony periphery for colonies developed on LB medium (n=6). Boxes represent Q1–Q3, lines represent the median, small squares represent the mean and bars span from max to min.

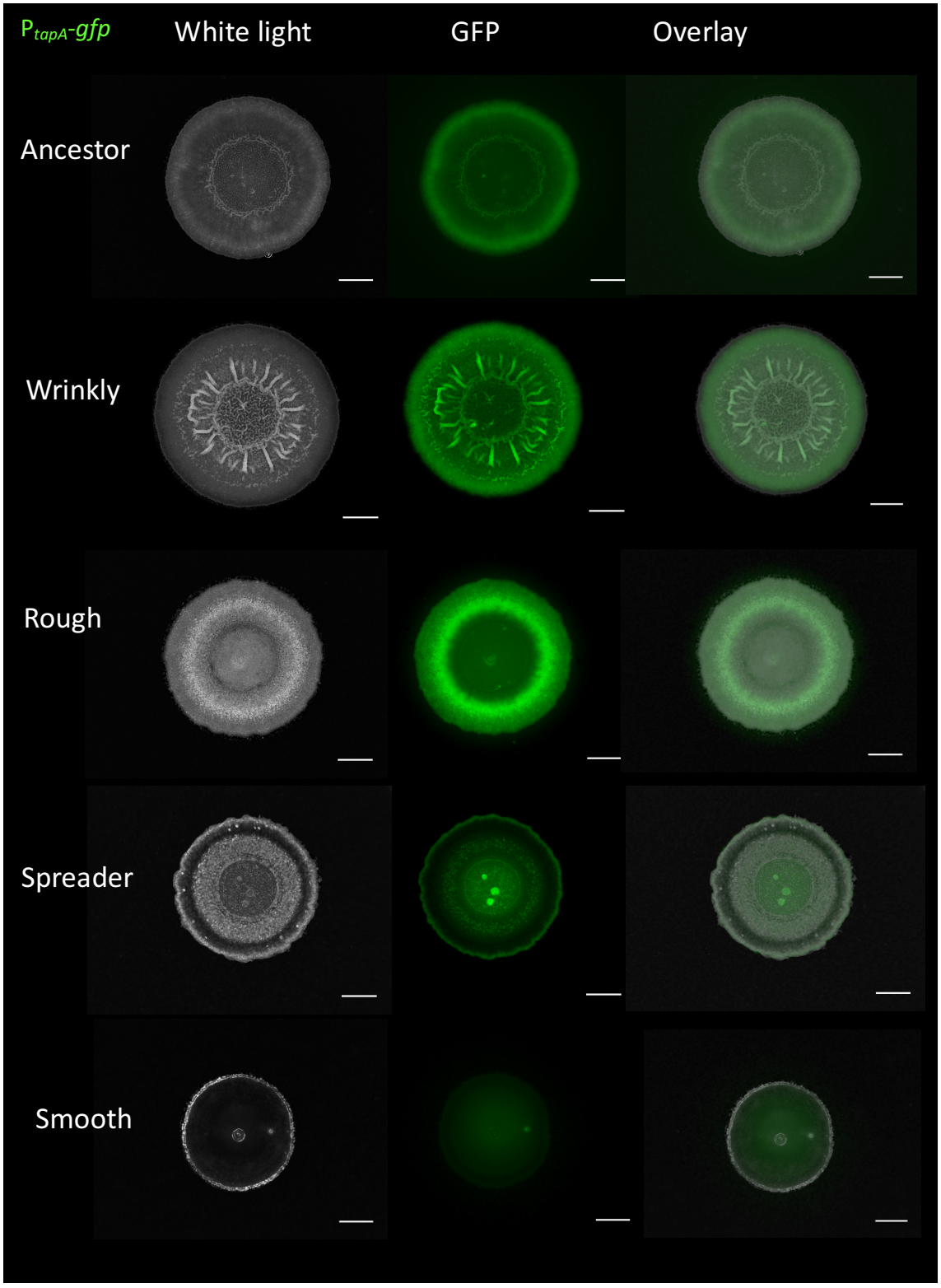

Supplementary Figure S3. Qualitative comparison of matrix-genes expression by different morphotypes. Expression of *eps* was monitored in the ancestor and all morphotypes in colonies developed on MSgg using P_{tapA}-*gfp* reporter fusion. Scale bar represents 2mm.

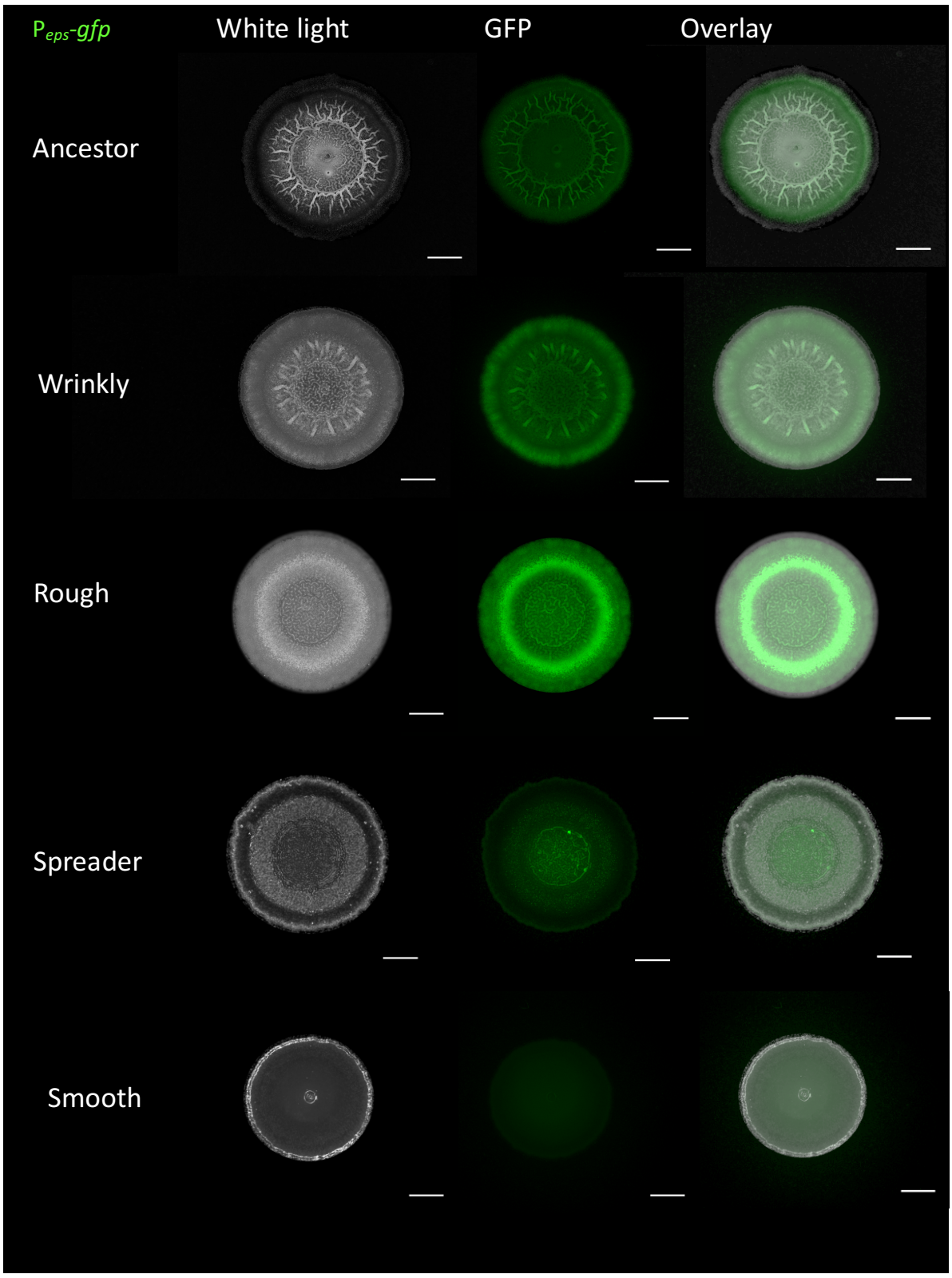

Supplementary Figure S4. Qualitative comparison of matrix-genes expression by different morphotypes. Expression of *tapA* was monitored in the ancestor and all morphotypes in colonies developed on MSgg using P_{eps}-*gfp* reporter fusion. Scale bar represents 2mm.

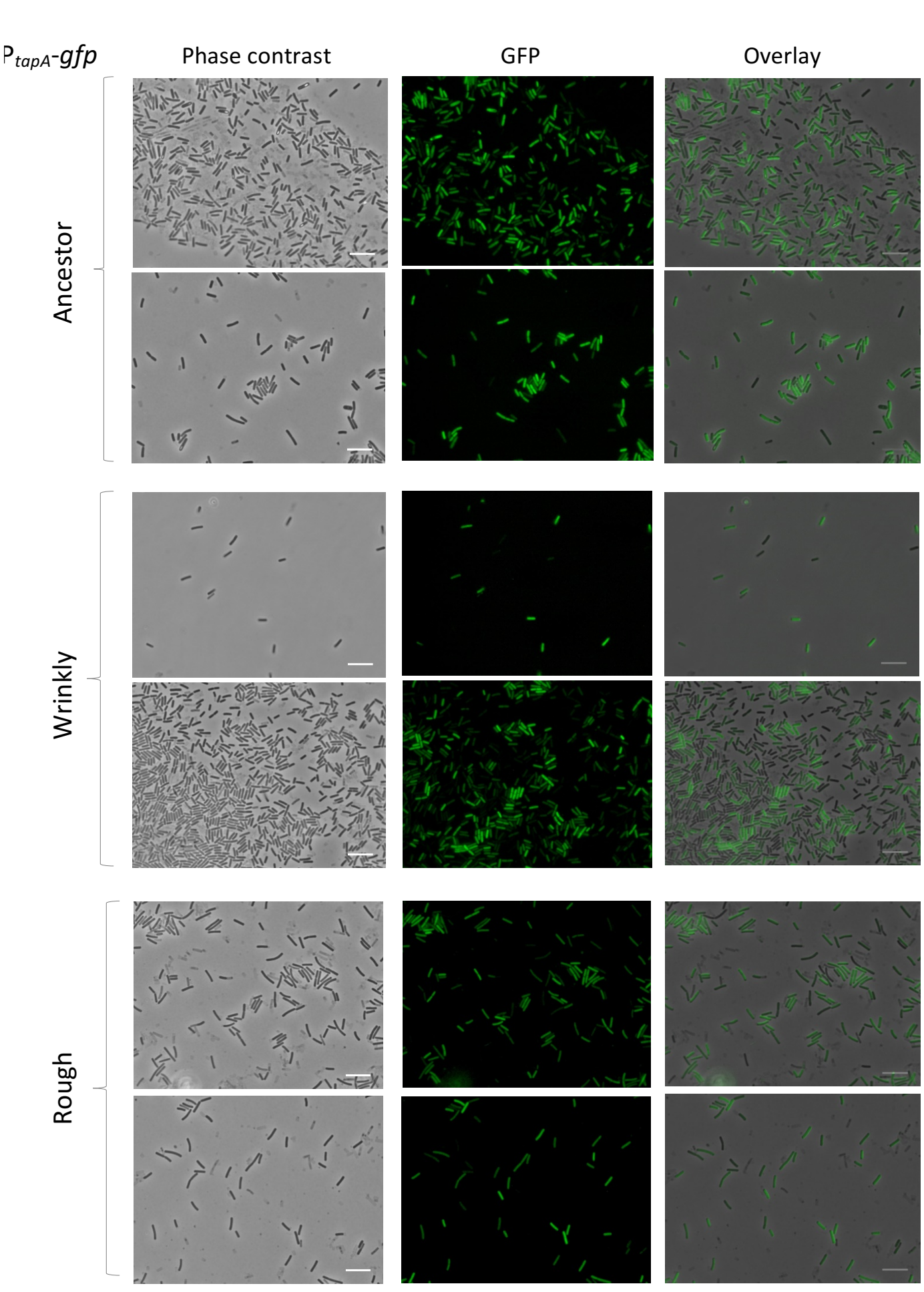
P_{tapA}-*gfp*
Phase contrast
GFP
Overlay
Ancestor
Wrinkly
Rough

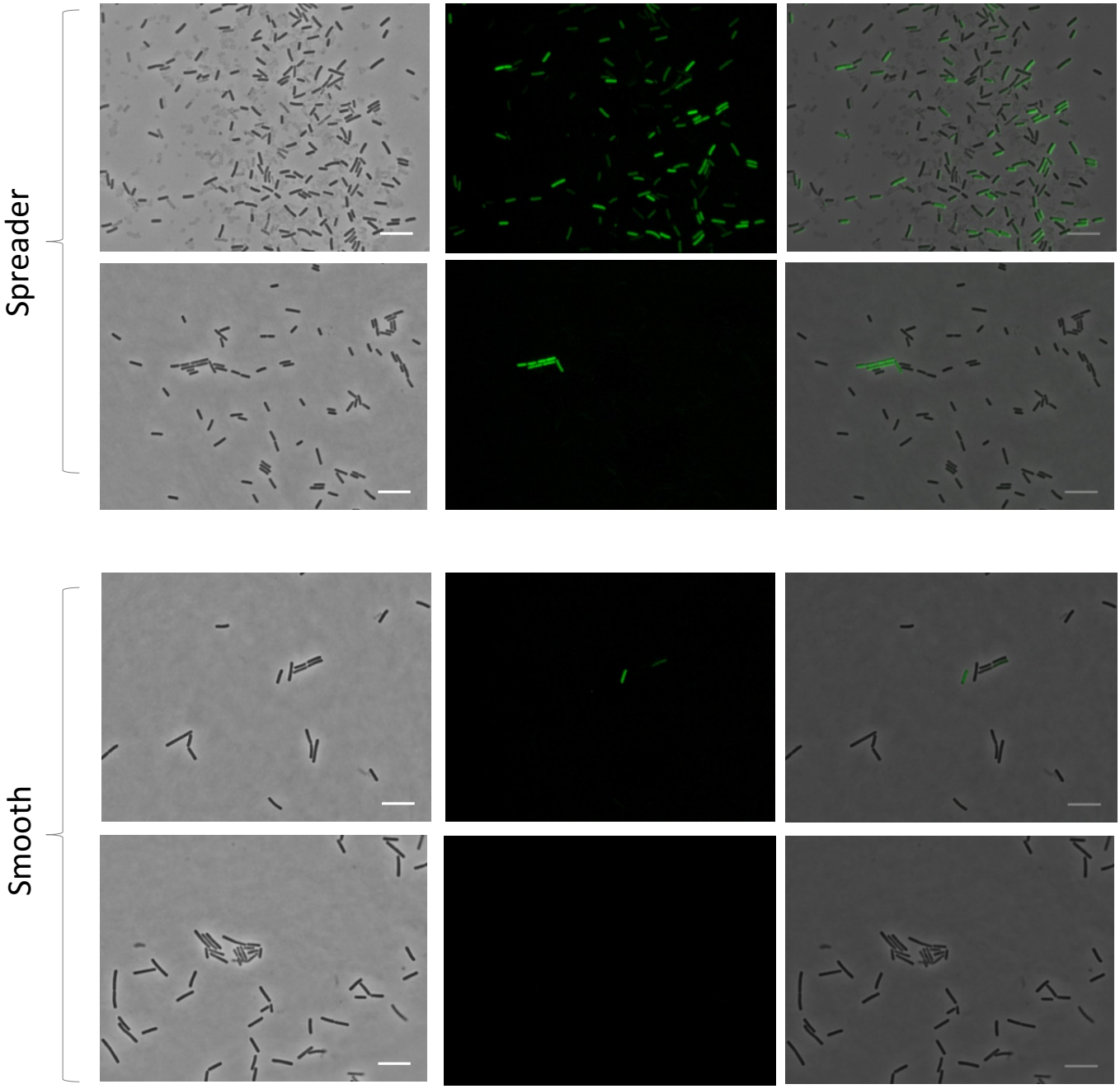

Supplemenatary Figure S5. Single-cell level expression of *tapA* in the ancestor and evolved morphotypes. The expression of P_{tapA}-*gfp* at single cell level was compared using epifluorescence. Pellicles were grown in MSgg medium at 30°C for 24 hours, harvested and disrupted to single-cell level by sonication. Time point 24h was selected, based on spectrofluorimetric analysis, as showing high differences in P*tapA* expression among morphotypes (Fig. 3A). Images taken from two independent biological replicates are presented for each morphotype. Scale bar corresponds to 10µm.

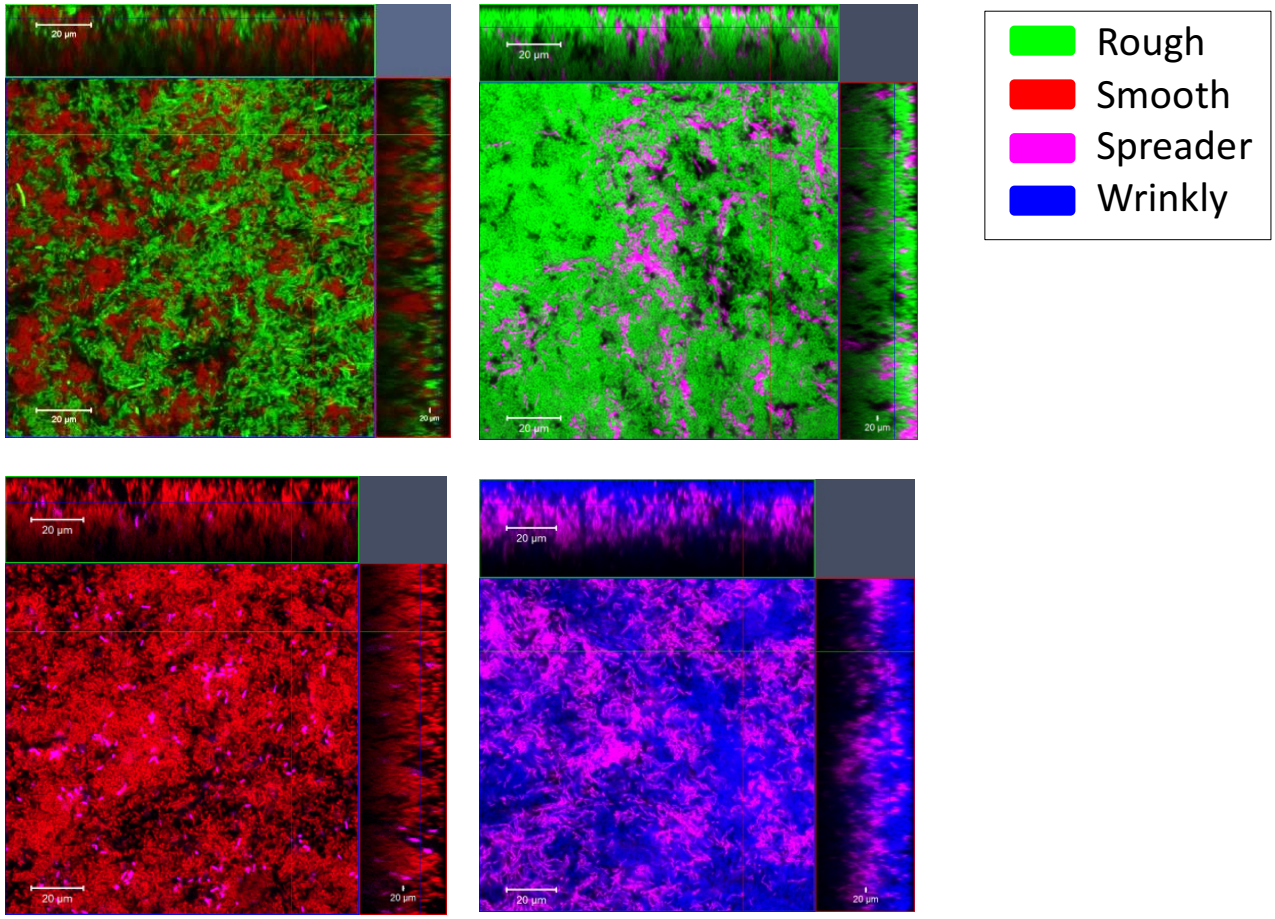

Supplementary Figure S6. Control experiments with swapped fluorescent markers for estimating the spatial assortment of morphotypes in the pellicles. Confocal microscopy images of pellicle biofilms formed by the mix of four morphotypes were taken. Each time only 2 selected morphotypes were labelled with constitutive fluorescent reporters and could be visualized in the pellicle. Morphotypes were mixed in ratios 0.9: 5.3:0.6:3.2 ratios and pellicle were allowed to form for 48h at 30°C. To simplify image comparison, each morphotype was artificially labelled with the same assigned color (regardless on actual fluorescent marker used) across all images: Rough – green, Smooth – red, Spreader – purple, Wrinkly - blue. The actual mixed cultures were: $Rough_{GFP}$ + $Smooth_{mKate}$ (+Wrinkly and Spreader unlabeled), $Rough_{mKate}$ + $Spreader_{GFP}$ (+Wrinkly and Smooth unlabeled), $Smooth_{mKate}$ + $Spreader_{GFP}$ (+Rough and Wrinkly unlabeled), $Spreader_{mKate}$ + $Wrinkly_{GFP}$ (+Rough and Smooth unlabeled).

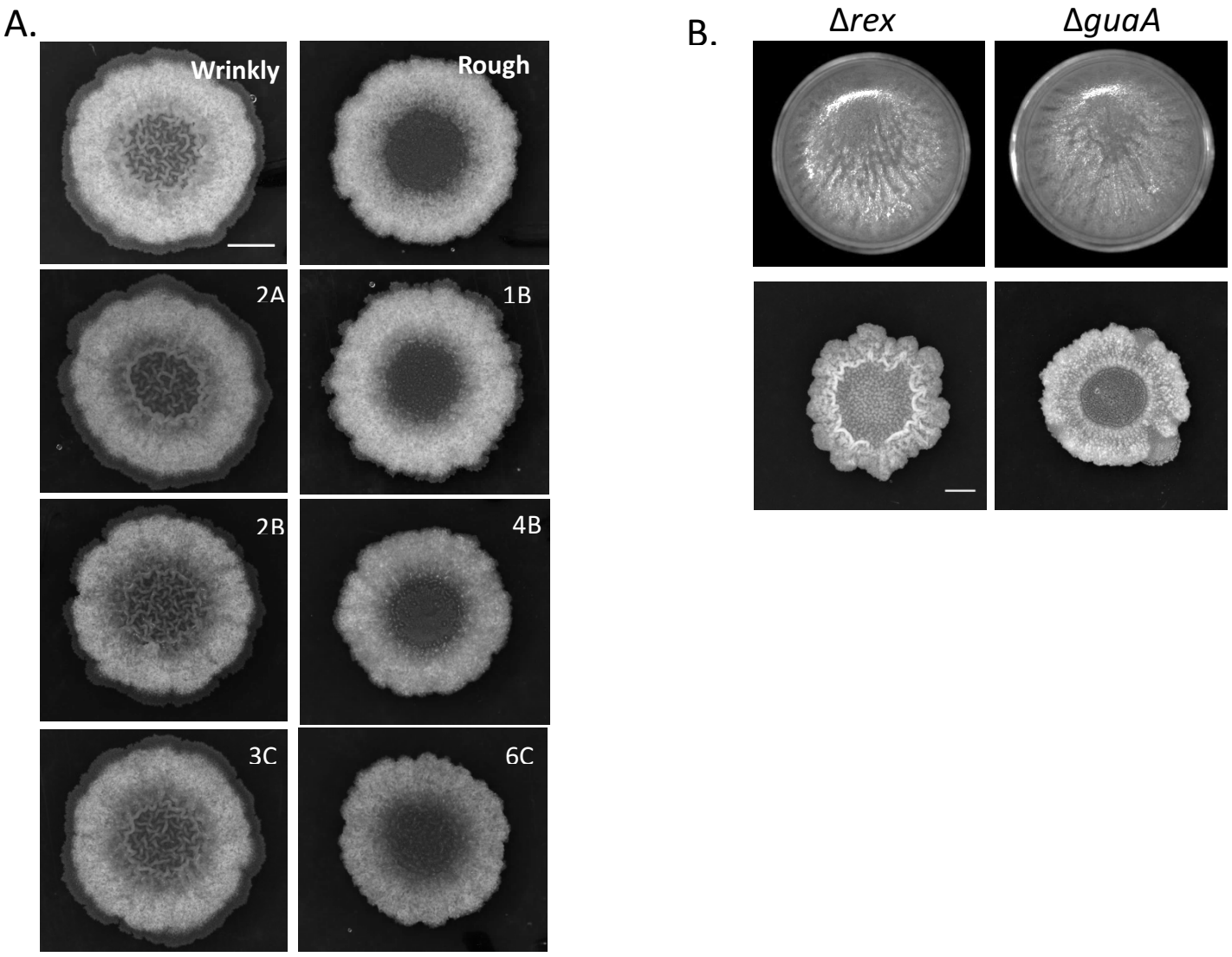

Supplementary Figure S7. Exploring molecular evolution pattern during diversification. **(A)** Morphologies of randomly picked colonies from populations 2-6 were evaluated and assigned to Wrinkly or Rough category based on similarity to those morphotypes from population 1. Isolates were subjected to whole- genome sequencing together with all morphotypes from population 1. Scale bar represents 2 mm. **(B)** Pellicle and colony morphologies of the ancestor strain carrying *rex* and *guaA* knockout strains. Pellicles and colonies were grown for 48h at 30°C. Well diameter is 1.5 cm. Scale bar represents 1 mm.

Strain name	Genotype	Reference
DK1042	NCIB 3610 *comI*^{Q12I}	Konkol, Blair and Kearns 2013
NRS2243	3610 *sacI::*P$_{eps}$-*gfp* (Km^{R})	Murray, Strauch and Stanley-Wall 2009
NRS2394	3610 *sacI::*P$_{tapA}$-*gfp* (Km^{R})	Murray, Strauch and Stanley-Wall 2009
BKE12280	168 *rex::mls*	Koo *et al.* 2017
BKE06360	168 *guaA::mls*	Koo *et al.* 2017
168 hyGFP	168 *amyE*::P$_{hyperspank}$-GFP (Cm^{R})	van Gestel *et al.* 2014
168 hymKate	168 *amyE*::P$_{hyperspank}$-mKATE2 (Cm^{R})	van Gestel *et al.* 2014
DTUB18	comI Rough *sacI::*P$_{eps}$-*gfp* (Km^{R})	This work
DTUB19	3610 *comI*^{Q12I} Wrinkly *sacI::*P$_{eps}$-*gfp* (Km^{R})	This work
DTUB20	3610 *comI*^{Q12I} Spreader *sacI::*P$_{eps}$-*gfp* (Km^{R})	This work
DTUB21	3610 *comI*^{Q12I} Smooth *sacI::*P$_{eps}$-*gfp* (Km^{R})	This work
DTUB22	3610 *comI*^{Q12I} Rough *sacI::*P$_{tapA}$-*gfp* (Km^{R})	This work
DTUB23	3610 *comI*^{Q12I} Wrinkly *sacI::*P$_{tapA}$-*gfp* (Km^{R})	This work
DTUB24	3610 *comI*^{Q12I} Spreader *sacI::*P$_{tapA}$-*gfp* (Km^{R})	This work
DTUB25	3610 *comI*^{Q12I} Smooth *sacI::*P$_{tapA}$-*gfp* (Km^{R})	This work
DTUB10	3610 *comI*^{Q12I} Rough *amyE*::P$_{hyperspank}$-*gfp* (Cm^{R})	This work
DTUB11	3610 *comI*^{Q12I} Wrinkly *amyE*::P$_{hyperspank}$-*gfp* (Cm^{R})	This work
DTUB12	3610 *comI*^{Q12I} Spreader *amyE*::P$_{hyperspank}$-*gfp* (Cm^{R})	This work
DTUB13	3610 *comI*^{Q12I} Smooth *amyE*::P$_{hyperspank}$-*gfp* (Cm^{R})	This work
DTUB14	3610 *comI*^{Q12I} Rough *amyE*::P$_{hyperspank}$-*mKATE2* (Cm^{R})	This work
DTUB15	3610 *comI*^{Q12I} Wrinkly *amyE*::P$_{hyperspank}$-*mKATE2* (Cm^{R})	This work
DTUB16	3610 *comI*^{Q12I} Spreader *amyE*::P$_{hyperspank}$-*mKATE2* (Cm^{R})	This work
DTUB17	3610 *comI*^{Q12I} Smooth *amyE*::P$_{hyperspank}$-*mKATE2* (Cm^{R})	This work
TB963	3610 *comI*^{Q12I} *rex::mls*	This work
TB964	3610 *comI*^{Q12I} *guaA::mls*	This work

Supplementary Table S1. Strains that were used in this study. NCIB 3610 *comI*^{Q12I} served as an ancestral strain in evolution experiment. Strains carrying fluorescent fusions were used as a source of genomic DNA to transform the evolved colony types. Strains DTU18-21 were obtained by transforming the evolved morphotypes with gDNA obtained from NRS2243. Strains DTU22-25 were obtained by transforming the evolved morphotypes with gDNA obtained from NRS2394. Strains DTUB10-B13 were obtained by transforming the evolved morphotypes with gDNA obtained from 168hyGFP. Strains DTUB14-B17 were obtained by transforming the evolved morphotypes with gDNA obtained from 168hymKate. Strains lacking *rex* and *guaA* were used as a source of gDNA to transform the ancestral strain in order to test for phenotypic effects of those mutations. TB963 and TB964 were obtained by transforming the DK1042 with gDNA obtained from BKE12280 and BKE06360, respectively.

REFERENCES

van Gestel J, Weissing FJ, Kuipers OP *et al.* Density of founder cells affects spatial pattern formation and cooperation in *Bacillus subtilis* biofilms. *ISME J* 2014;**8**:2069–2079.

Konkol MA, Blair KM, Kearns DB. Plasmid-encoded ComI inhibits competence in the ancestral 3610 Strain of *Bacillus subtilis*. *J Bacteriol* 2013;**195**:4085–4093.

Koo B-M, Kritikos G, Farelli JD *et al.* Construction and analysis of two genome-scale deletion libraries for *Bacillus subtilis*. *Cell Syst* 2017;**4**:291–305.

Murray EJ, Strauch MA, Stanley-Wall NR. SigmaX is involved in controlling *Bacillus subtilis* biofilm architecture through the AbrB homologue Abh. *J Bacteriol* 2009;**191**:6822-6832.

Strain	Av. Coverage	Av. Freq. of mutation [%]	mutations with freq.<50% [%]
Ancestor	174.05	97.4	0.05
Wrinkly 1	150.14	92.3	0.06
Wrinkly 2A	145.22	92.4	0.06
Wrinkly 2B	360.2	93.2	0.06
Wrinkly 3C	552.05	92.5	0.07
Rough 1	214.88	93.9	0.006
Rough 1B	131.66	92.8	0.05
Rough 4B	305.72	92.8	0.06
Rough 6C	218.4	91.8	0.07
Spreader	172.54	93.1	0.06
Smooth	156.4	93.8	0.037

Supplementary Table S2. Sequencing statistics. The table lists following parameters: Average coverage per genome obtained for each strain that was sequenced in the study; Average frequency of detected mutation (SNP or InDel) per genome (with 25% of variant calling frequency); Percent of detected mutations with frequency lower than 50%.

Population	r^2 (0-24#)	p-value (0-24#)	r^2 (0-24#)	p-value (0-35#)
1	0.51	0.11	0.27	0.24
2	0.41	0.17	0.48	0.09
3	0.61	0.07	0.34	0.17
4	**0.79**	**0.02**	0.52	0.07
5	0.37	0.20	0.35	0.16
6	0.38	0.19	0.00	0.99
All populations	**0.35**	**0.0001**	**0.24**	**0.0009**

Supplementary Table S3. Regression analysis of productivity changes during evolution. Changes of productivity thorough an evolutionary time for each population separately and together for all populations were statistically accessed using regression analysis. The analysis was performed with and without the final time point 35# where productivity dropped for all populations. R-squared (r^2) values correspond to proportion of variation explained by linear model. Statistically significant results ($p<0.05$) are highlighted in green.

	Pop 1	Pop 2	Pop 3	Pop 4	Pop 5	Pop 6
Pop 1	1					
Pop 2	0.87	1				
Pop 3	0.95	0.91	1			
Pop 4	0.87	0.88	0.96	1		
Pop 5	0.75	0.86	0.82	0.83	1	
Pop 6	0.43	0.37	0.55	0.57	0.57	1

Supplementary Table S4. Synchrony in productivity changes across evolutionary time in all 6 independently evolved populations accessed using correlation test. Pair-wise comparison was performed for all possible combinations and the obtained values of Pearson's correlation coefficients r were presented in the table. In most cases (with an exception of Population 6) r values are very high ($r>0.8$) indicating synchronous productivity changes across the populations.

Single Factor ANOVA			
	F	*p-value*	*F critical*
Smooth	**11.5**	**0.0003**	**3.11**
Rough	4.27	0.02	3.11
Wrinkly	0.75	0.60	3.11
Spreader	1.83	0.18	3.11

Student's t test - Smooth%						
	Pop 1	Pop 2	Pop 3	Pop 4	Pop 5	Pop 6
Pop 1						
Pop 2	**0.01**					
Pop 3	**0.05**	0.91				
Pop 4	**0.009**	0.22	0.48			
Pop 5	**0.02**	0.77	0.98	0.20		
Pop 6	0.59	**0.003**	**0.02**	**0.002**	**0.005**	

Student's t test - Rough%						
	Pop 1	Pop 2	Pop 3	Pop 4	Pop 5	Pop 6
Pop 1						
Pop 2	**0.002**					
Pop 3	0.21	0.60				
Pop 4	**0.003**	0.78	0.57			
Pop 5	0.16	0.50	0.97	0.47		
Pop 6	0.16	**0.0001**	0.11	**0.0004**	0.07	

Supplementary Table S5. Differences in distribution of 4 morphotypes (Wrinkly, Rough, Spreader and Smooth) across 6 independently evolved populations at final #35 evolutionary timepoint. According to Benferroni adjusted p-value for the above single factor ANOVA (N=15; adjusted p-value<0.003), we detect statistically significant differences between the populations with respect to percent of Smooth morphotype. Student's t test further revealed that Population 1 and 6 were significantly differed from other populations in percentage of Smooth morphotype ($p<0.05$). Consistently, the Populations 1 and 6 showed the lowest p-values when percentage of Rough morphotype was compared with other populations.